

## Journal of Nanoscience with Advanced Technology

### Fabrication and Characteristics of the Reactive Sputtered Ta-N Thin Films with Ti Addition

Chung CK\*, Chang NW and Chen TS

Department of Mechanical Engineering, National Cheng Kung University, Tainan701, Taiwan

**\*Corresponding author:** Chung CK, Department of Mechanical Engineering, National Cheng Kung University, Tainan 701, Taiwan; Tel: +886-6-2757575-62111; Fax: +886-6-2352973; E mail: ckchung@mail.ncku.edu.tw

**Article Type:** Short Communication, **Submission Date:** 05 March 2018, **Accepted Date:** 20 March 2018, **Published Date:** 10 April 2018.

**Citation:** Chung CK, Chang NW and Chen TS (2018) Fabrication and Characteristics of the Reactive Sputtered Ta-N Thin Films with Ti Addition. *J Nanosci Adv Tech* 2(3): 1-5.

**Copyright:** © 2018 Chung CK, et al. This is an open-access article distributed under the terms of the Creative Commons Attribution License, which permits unrestricted use, distribution, and reproduction in any medium, provided the original author and source are credited.

#### Abstract

The combination of Ta-N and Ti-N is expected to create a range of multi-functional materials because of the composition dependent resistivity and thermal coefficient of resistance for the applications in micro-electronics and thermal sensors industry. In this article, adding Ti into the Ta-N thin film has been investigated by various sputtering conditions to create the possibility with varied electrical property which can be good for resistor and sensor application. A series of Ta-N (0Ti%) and Ta-Ti-N thin films were deposited by DC magnetron sputtering. The microstructure, composition, morphology and electrical properties of the films were characterized using X-ray diffraction (XRD), energy-dispersive X-ray spectroscopy, scanning electron microscopy and four point probe method. The crystal structures of Ta, Ti and Ta-Ti alloys are based on bcc  $\alpha$ -Ta and bcc  $\beta$ -Ti. XRD patterns showed Ta-N is quasi-amorphous structure with high  $N_2$  flow ratio of 20% while Ta-Ti-N is preferred to form polycrystalline phase. The resistivity of both kinds of thin films decreases with increasing temperatures for the nature of negative temperature coefficient of resistance (N-TCR). The magnitude of both resistivity and N-TCR increases with increasing  $N_2$  flow ratio. The wide range of resistivity and TCR can be used for applications in thermally based micro sensors (high TCR) and thin-film resistor (low TCR).

**Keywords:** Thin film, Ta-Ti-N, Sputtering, TCR, Resistor, Sensor.

#### Introduction

Copper has been extensively studied as a potential substitute for aluminum and aluminum alloy due to its lower bulk resistance and excellent electro-migration resistance. It is well known that copper is a faster diffuser in Si and  $SiO_2$ , which makes diffusion barrier layer so important in Cu metallization [1-2]. The tantalum (Ta) and tantalum nitride (TaN) [3] barrier layers have been widely used as diffusion barriers and thin film resistors in the microelectronics industry due to their good diffusion barrier

properties [1,4,5] and relatively stable electrical properties [6-8]. TiN have also received much attention as diffusion barrier [9-11] due to its mechanical stability [9,12] and low resistivity [10,11]. Furthermore, multi-component composite coatings, multi-layer coatings and super-lattice coatings have been introduced [6,13-16]. It shows the possibility of ternary material work for diffusion barrier. If the third element is also a transition metal, a solid solution with crystal structure and electronic properties similar to the original nitride may form. Compared to those of the constituting binary nitrides, solid solutions were found to possess better performance [17]. The multi-component alloy has already become one of the most attractive biomaterials. The other metallic biomaterials Ti-Ta alloys are expected to be promising biomaterials due to their superior comprehensive properties. But only few experimental investigations have been focus on Ta content on the modulus and strength of binary Ti-Ta alloys [18-20]. The metallurgical practices have proven that alloying can improve the mechanical properties over either of its constituent pure metals, but the large difference in the melting points (Ti: 1953 K, Ta: 3273 K) and the densities (Ti: 4.51 g/cm<sup>3</sup>, Ta: 16.6 g/cm<sup>3</sup>) of Ti and Ta in their pure state result in the difficulty of melting operation [18].

Tantalum nitride thin films are a promising material for a high accuracy embedded thin-film resistor (TFR) [21] in electronic and optical devices to make a light, thin, short and small product with small tolerance. A low or near-zero temperature coefficient of resistance (TCR) is also required for the high reliability of TFR. Ta and Ta-N Ta-Ta-N have been developed for an embedded resistor with high accuracy [22]. Low resistivity and low temperature coefficient of resistance TCR, which guarantee low and constant electric resistance over a wide range of temperature, are required in microelectronics, especially in portable terminal or telecommunication devices, for the purpose of saving the consumption of batteries [23]. In the application of thermal resistive sensors [24], resolution is mainly dependent

on the sensing material's TCR and resistivity, while accuracy depends on linearity of resistance variation with temperature. The high TCR is generally beneficial for the sensitivity of sensor.

In this work, thin films were deposited by direct current reactive magnetron co-sputtering as a deposition technique. It will overcome the mixing problem and give the possibility to control the property in simple way. The electrical resistivity and structure properties were investigated between Ti participation and different N<sub>2</sub> sputtering gas condition of thin films. The relationship between process, microstructure, resistivity and TCR of thin films was discussed and established.

### Experimental details

Boron-doped p-Si (100) wafers of 4-10 Ω-cm were initially cleaned in a solution of H<sub>2</sub>SO<sub>4</sub> and H<sub>2</sub>O<sub>2</sub> (3:1). The wafers were placed into an oxidation furnace at 1000 °C in order to grow the thermal oxide layer as an insulator layer. The thin films were deposited by direct-current (DC) reactive sputtering with a pure tantalum target (99.99% purity) and pure titanium target (99.99% purity). The targets were cleaned by pre-sputtering process in Ar plasma. A shutter placed between the magnetron and the substrate holder allowed the machine controlled the sputtering time at 30 min and pre-clean target before the film deposition for 10 min. The DC power was fixed at 50 W. The nitrogen flow ratio (FN<sub>2</sub>% = FN<sub>2</sub> / (F<sub>Ar</sub> + FN<sub>2</sub>) × 100%) controlled between 0% to 20% keeps total flow rate at 100 sccm by mass flow controller. The base pressure was controlled at 8 × 10<sup>-4</sup> Pa and working pressure was 53.32 Pa. The substrate holder was rotated at 35 rpm (revolution per minute) to improve the deposition uniformity without any additional cooling or heating. The phases and microstructure of Ta-(Ti)-N films were characterized by grazing incidence X-ray Diffractometer (GIXRD, D/MAX2500, RIGAKU, Japan) with an incident angle of 2° using Cu Kα radiation (0.15418 nm). The morphology of thin films was examined by field-emission scanning electron microscopy (FESEM, JSM-6700F, JEOL, Japan). The composition of Ta-N films was analyzed by

energy dispersive spectrometry (EDS, INCA 400) attached to FESEM. The electric resistivity and TCR of Ta-(Ti)-N films were measured by four-point probe method with the Keithley 2400 current-voltage meters and heated by hotplate. The resistivity is measured at room temperature (25°C) while the TCR is obtained in a range of 30-100°C.

### Results and discussion

Figure 1 shows the GIXRD patterns of the as-deposited Ta-N films at FN<sub>2</sub>% = 0, 5, 10 and 20% without substrate heating or bias adding at the fixed 50 W Ta power. The possible crystalline of Ta and Ta-N compounds in JCPDS numbers are α-Ta (body-centered cubic, BCC, No. 04-0788) and TaN (face-centered cubic, FCC, No. 32-1283). The main diffraction planes from each phase are denoted by the black points for identifying the crystallization. Pure Ta deposited at 0 FN<sub>2</sub>%, only polycrystalline α-Ta is detected with three distinct (110), (200) and (211) diffraction peaks at 2θ = 38.47°, 55.54° and 69.58°. The TaN films was observed with five sharp diffracted peaks from the (111), (200), (220), (311) and (220) planes at FN<sub>2</sub>% = 5~10%. The N-rich TaN phase was found with a broad peaks from 28~38° at FN<sub>2</sub>% = 20%. The symmetrical broad peak with a large FWHM implies nanocrystalline grains embedded in an amorphous matrix to form an amorphous-like microstructure. In the other hand, the several steep peaks with small FWHM indicate that the structure is polycrystalline. The relative high N<sub>2</sub> ratio reduces the reactive plasma energy which makes the recrystallization unable to work on the surface, and also causes the deposition rate drop from 6.3 nm to 4.4 nm per minute. With Ti element adding as a substitution solid solution the diffraction patterns is similar result to TaN. Ti structure is closed to Ta because there lattice number quit same (3.3065Å and 3.3058Å). Moreover, in JCPDS numbers β-Ti (body-centered cubic, BCC, No. 44-1288) and TiN (face-centered cubic, FCC, No. 38-1420) shows almost the same diffraction peaks position with tiny degree shifting. The SEM micrographs in Figure 2 show evolution of thin film

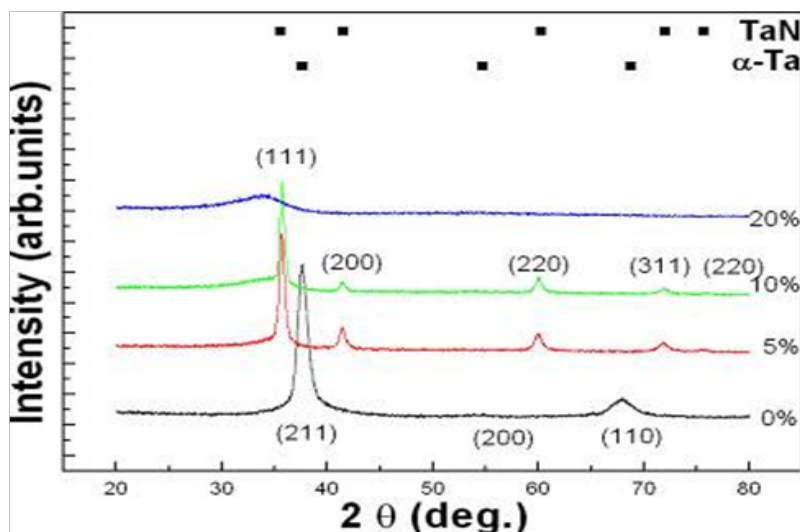


Figure 1: XRD pattern of Ta-N films at FN2%= 0, 5, 10 and 20%

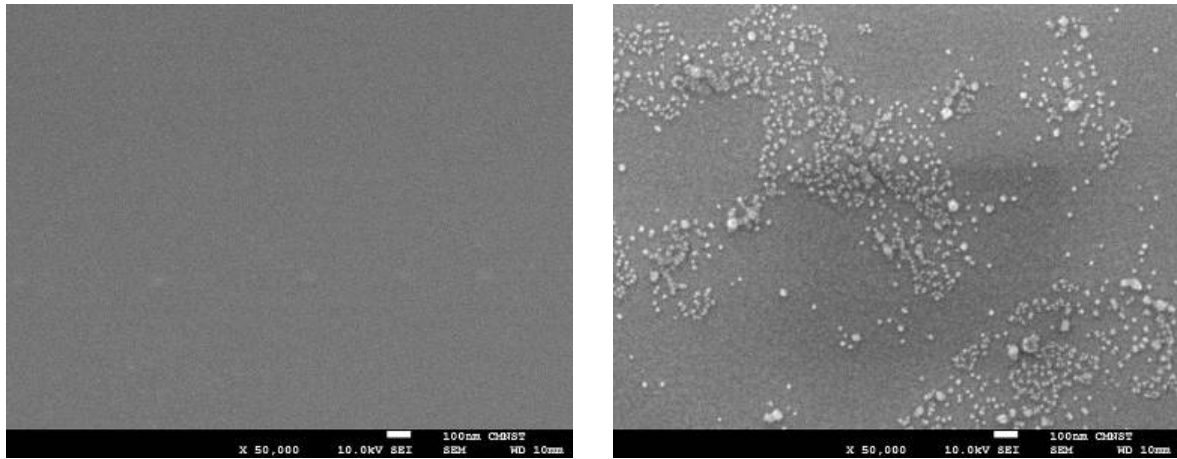


Figure 2: SEM surface morphology of the samples: (a) Ta and (b) Ta-Ti-N at FN<sub>2</sub>%= 20%

morphology. The Ta film shows smooth morphology and closer boundary arrangement (Figure 2(a)). With Ti adding and sputtering at FN<sub>2</sub>%= 20%, some particles from precipitation are formed on the surface. It may be attributed that both Ta-N and Ti-N have some mismatch and increases surface energy to make incomplete solid solution.

The evolution of microstructure, phase and morphology can influence the electrical properties of Ta-(Ti)-N films as shown in Figure 3 (a) and (b), respectively.

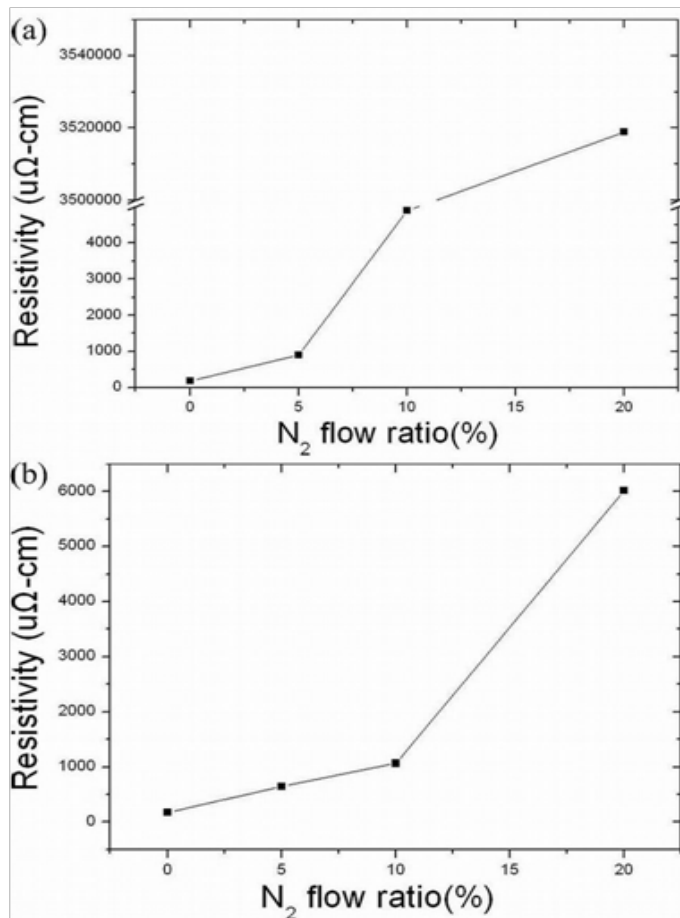


Figure 3: Influence of deposition gas on the resistivity of: (a) Ta-N films (b) Ta-Ti-N at FN<sub>2</sub>%= 0, 5, 10 and 20%. The resistivity is measured at

room temperature (25°C)

The EDS measured composition (at%) and resistivity of Ta-Ti-N films at different FN<sub>2</sub>% are listed in Table.

**Table:** The EDS measured composition (at%) and resistivity of Ta-Ti-N films at different FN<sub>2</sub>%. The resistivity is measured at room temperature (25°C)

Nitrogen flow rate (%)	Composition (at %)				Resistivity (μΩ cm)
	Ta	Ti	N/Ta	N/Ti	
0	73.8	12.5	0	0	1.8×10 <sup>2</sup>
5	61.4	7.6	0.31	2.47	6.5×10 <sup>2</sup>
10	59.8	6.5	0.41	3.83	1.1×10 <sup>3</sup>
20	57.3	7.6	0.47	3.54	6.0×10 <sup>3</sup>

The electrical resistivity of Ta-N films increases with increasing FN<sub>2</sub>%. The resistivity of polycrystalline film at FN<sub>2</sub>%= 0~10% is around 186~4.9×10<sup>4</sup>μΩ cm while the nanocomposite amorphous films at 20% is high up to 3.9 ×10<sup>6</sup>μΩ cm. As above mention, the pure Ta film's shows polycrystalline α-Ta structure. In the previous research, α-Ta (body-center cubic) has low resistivity of 15~60 μΩ-cm and the β-phase Ta (metastable tetragonal) has higher resistivity of 150~210 μΩ-cm [25]. The oxygen trapped inside thin films and caused the interrupt of the electron path. This maybe the reason cause resistivity increases up to the range of β-Ta but still maintain α- Ta structure. The low resistivity of Ta-N films is primarily from more metallic bonding rather than the ionic/covalent bonding. Therefore, the majority of carriers in the conducting Ta-N films are electrons. The increase of electrical resistivity is attributed to the reduced mobility and density of electrons in different microstructures and compositions. The electron mobility is related to the electronic scattering and tunneling at grain boundary (GB), grain size (*D*), inner-crystalline mean free path (*L*) as well as GB tunneling probability (*G*) of electrons. According to the grain boundary scattering model [26,27] (valid in the limit of *L/D*>1), especially for a nanocomposite amorphous material with tiny *D* which is significantly smaller than *L* the dc electrical resistivity (*ρ*) can be expressed by the equation  $\rho = K/(LG^{L/D})$ , where *K* is



material-dependent constant related to the effective mass, Fermi velocity and density of carriers. The  $LG^{L/D}$  can be represented by an effective mean free path ( $L_G$ ),  $L_G = LG^{L/D}$  to describe the electron scattering including the grain-size effect. The structure transform for Ta-N with  $FN_2\% = 20\%$  leads to the  $L_G$  reduction and resistivity dramatic increase. On the contrast, the Ta-Ti-N shows the steady increase resistivity due to the increase of ionic-covalent bonding.

The other important property is temperature coefficient of resistance (TCR). The resistivity decreases with increasing temperature, which is the characteristic of negative TCR. TCR (ppm/°C) is defined as

$$TCR \text{ (ppm/}^\circ\text{C)} = [(\rho_2 - \rho_1) / \rho_1 (T_2 - T_1)] \times 10^6 \quad (1)$$

$\rho_1$  and  $\rho_2$  are the resistivity at temperatures  $T_1$  and  $T_2$ . TCR has been determined for the temperature range from 30 °C to 100 °C where the result varied linearly with  $FN_2\%$ . Most pure metals have positive TCRs of several thousand ppm/°C. Negative TCRs occur in several amorphous alloys, semiconductor materials and metastable crystalline states. Higher temperature with larger tunneling probability results in lower resistivity for negative temperature coefficient of resistance which is a non-metallic behavior and found in other sputtered transition metal nitrides.

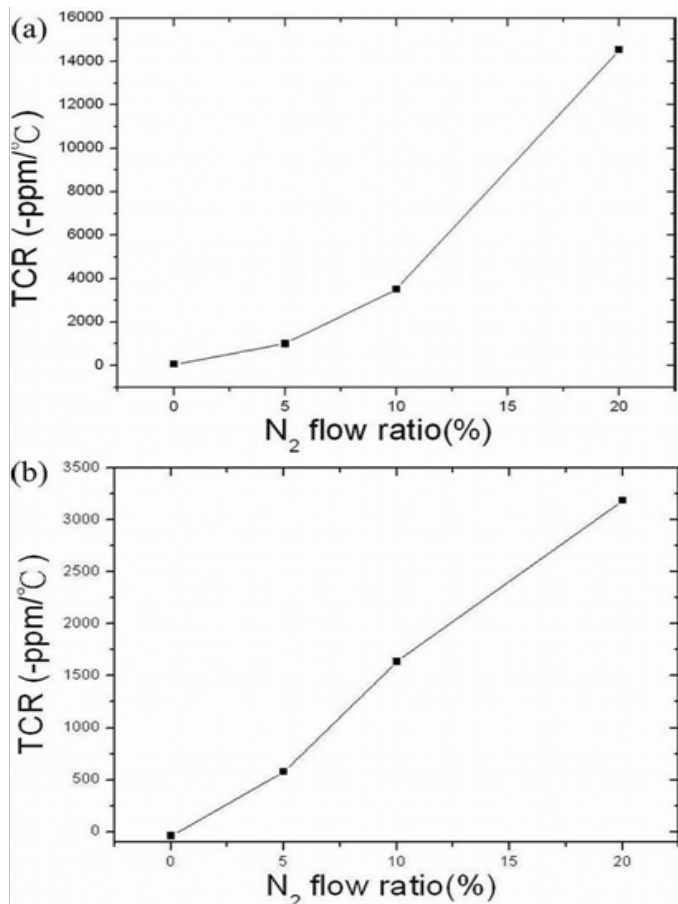


**Figure 4:** The TCR of: (a) Ta-N films (b) Ta-N with Ti adding (Ta-Ti-N) at  $FN_2\% = 0, 5, 10$  and  $20\%$

Figure 4 shows the Ta-N films and Ta-Ti-N exhibit the negative TCR behavior, which increases with  $FN_2\%$  around  $-55$  to  $-1.4 \times 10^4$

ppm/°C. The highest resistivity ( $3.9 \times 10^6 \mu\Omega$ ) cm and negative TCR ( $-1.4 \times 10^4$  ppm/°C) are obtained at TaN thin film  $FN_2\% = 20\%$ . But the nonlinear properties may not good for electrical application. From Figure 4(b), the TCR for Ta-Ti-N shows linear decrease to  $-3.1 \times 10^3$  ppm/°C with increasing  $FN_2\%$ . The stable polycrystalline structure maybe the reason why TCR linearly decreasing.

TaN film shows a high resistivity and huge N-TCR change but nonlinear property may not good for application. The addition of Ti maintains the crystal structure. This make the thin films electrical property can simply controlled by  $FN_2\%$ . Figure 4(b) shows the stable decrease TCR from  $-39$  to  $-3.1 \times 10^3$  ppm/°C for Ta-Ti-N. This means only the  $FN_2\%$  involve the change of TCR. In the other word, the Ta-Ti-N films can precise control the TCR because the poly-crystal structure is stable. The results showed that Ta-Ti-N film at high  $FN_2\%$  possessed a high resistivity and high negative coefficient of resistance (N-TCR), which may be recognized as the best properties for application in thermally based micro sensors. Ta-Ti films which can precisely control the electrical property may be suitable for thin-film resistor.

### Conclusion

The effect of Ti addition on microstructure and electrical properties of Ta-(Ti)-N films have been studied. Experiment result shows possibility to form alloy nitride even the large difference in the melting points and the densities. The resistivity and TCR of Ta-(Ti)-N films are related to the evolution of microstructure, phase and composition at various  $FN_2\%$ . The Ta and Ti ratio decreases with increasing  $FN_2\%$  while the  $N_2$  ratio increases inversely. Accordingly, both resistivity and TCR increase with increasing  $FN_2\%$ . The increase of nitrogen contents leads to the increasing of ionic-covalent bond (Ta-N and Ti-N). The reduced free electron density and mobility increase resistivity. Totally, the higher the resistivity goes with the larger gradient of TCR because the ionic-covalent bond increasing. The great increase of TCR in Ta-N films at high  $FN_2\%$  was attributed to the quasi-amorphous microstructure. The adding of Ti maintains the polycrystalline structure. Without the amorphous structure effect, the Ta-(Ti)-N thin films electrical property keeps in stable change with  $FN_2\%$ . Ta-Ti-N film deposited at various  $FN_2\%$  shows the relative low resistivity form  $176 \sim 6.0 \times 10^3 \mu\Omega$  cm and negative TCR from  $-39$  to  $-3.1 \times 10^3$  ppm/°C. In addition, Ta-Ti-N film at high  $FN_2\%$  possessed a high resistivity and high negative coefficient of resistance (N-TCR), which may be recognized as the best properties for application in thermally based micro sensors. Ta-Ti films which can precisely control the electrical property may be suitable for thin-film resistor.

### Acknowledgements

This work is partially sponsored by Ministry of Science and Technology, Taiwan, under contract No MOST 106-2221-E-006-101-MY3. We pay our great thanks to the Center for Micro/Nano Science and Technology (CMNST) in National Cheng Kung University for the access of process and analysis equipment's.

## References

1. Yang L, Zhang D, Li C, Liu R, Lu P, Foo P, et al. *Thin Solid Films*. 2006; 504:265-268.
2. Hsieh JH, Cheng MK, Li C, Chen SH, Chang YG. *Thin Solid Films*. 2008; 516:5430-5434.
3. Lee WH, Lin JC, Lee C. *Materials Chemistry and Physics*. 2001; 68:266-271.
4. Xie Q, Qu XP, Tan JJ, Jiang YL, Zhou M, Chen T, et al. *Applied Surface Science*. 2006; 253:1666-1672.
5. Hübner R, Hecker M, Mattern N, Hoffmann V, Wetzig K, Wenger C, et al. *Thin Solid Films*. 2003; 437:248-256.
6. Araujo RA, Yoon J, Zhang X, Wang H. *Thin Solid Films*. 2008; 516:5103-5106.
7. Kim J, Jo S. *Journal of Magnetism and Magnetic Materials*. 2008; 320:2116-2120.
8. Yuan ZL, Zhang DH, Li CY, Prasad K, Tan CM. *Thin Solid Films*. 2004; 462-463:284-287.
9. Alberti A, Molinaro S, La Via F, Bongiorno C, Ceriola G, Ravesi S. *Microelectronic Engineering*. 2002; 60:81-87.
10. Bonitz J, Schulz SE, Gessner T. *Microelectronic Engineering*. 2003; 70:330-336.
11. Deenamma Vargheese K, Mohan Rao G, Balasubramanian TV, Kumar S. *Materials Science and Engineering B*. 2001; 83:242-248.
12. Kaufmann C, Baumann J, Gessner T, Raschke T, Rennau M, Zichner N. *Applied Surface Science*. 1995; 91:291-294.
13. Chen YH, Lee KW, Chiou WA, Chung YW, Keer LM. *Surface and Coatings Technology*. 2011; 146-147:209-214.
14. Chung CK, Chang HC, Chang SC, Liao MW, Lai CC. *J. Alloys and Compounds*. 2012; 537:318-322.
15. Barshilia HC, Rajam KS. *Surface and Coatings Technology*. 2004; 183:174-183.
16. Ma KJ, Chao CL, Liu DS, Chen YT, Shieh MB. *Journal of Materials Processing Technology*. 2002; 127:182-186.
17. Feng W, Zhou H, Yang Sze. *Materials Chemistry and Physics*. 2010; 124:287-290.
18. Zhou YL, Niinomi M. *Materials Science and Engineering: C*. 2009; 29:1061-1065.
19. Zhou YL, Niinomi M, Akahori T, Fukui H, Toda H. *Materials Science and Engineering A*. 2005; 398:28-36.
20. Mareci D, Chelariu R, Gordin DM, Ungureanu G, Gloriant T. *Acta Biomaterialia*. 2009; 5:3625-3639.
21. Na SM, Park IS, Park SY, Jeong GH, Suh SJ. *Thin Solid Films*. 2008; 516:5465-5469.
22. Kang SM, Yoon SG, Suh SJ, Yoon DH. *Thin Solid Films*. 2008; 516:3568-3571.
23. Ishikawa M, Enomoto H, Mikamoto N, Nakamura T, Matsuoka M, Iwakura C. *Surface and Coatings Technology*. 1998; 110:121-127.
24. Chung CK, Chang YL, Wu JC, Jhu JJ, Chen TS. *Sensors and Actuators A: Physical*. 2009; 156:323-327.
25. Wang YS, Hung CC, Lee WH, Chang SC, Wang YL. *Thin Solid Films*. 2008; 516:5241-5243.
26. Sanjinés R, Benkahoul M, Sandu CS, Schmid PE, Lévy FJ. *Appl. Phys.* 2005; 98:123511.
27. Chung CK, Nautiyal A, Chen TS, Chang YL. *J. Phys. D: Appl. Phys.* 2008; 41:185404.